Autocorrelation functions for contour cuts through self-affine surfaces

Srinivasa B. Ramisetti,[1] Carlos Campañá,[2] Guillaume Anciaux,[1] Jean-Francois Molinari,[1] Martin H. Müser[2] and Mark O. Robbins[3]

[1]Ecole Polytechnique Fédérale de Lausanne, ENAC, Laboratoire de Simulation en Mécanique des Solides, 1015 Lausanne, Switzerland

[2]Lehrstuhl für Materialsimulation, Universität des Saarlandes, 66111 Saarbrücken, Germany

[3]Department of Physics and Astronomy, Johns Hopkins University, Baltimore, MD 21218, U.S.A.

E-mail: [3]mr@jhu.edu

Abstract. Regions between contours of constant height where the height is below the contour height are studied as a function of the Hurst exponent H. These contour cuts correspond directly to regions of mechanical contact in the common bearing area model for contact between self-affine surfaces. Regions below or above a given height also correspond to lakes or islands on a fractal landscape. The autocorrelation function $C(\Delta r)$ is defined as the probability that points separated by Δr are both within the contour cut. The scaling of C has important implications for the stiffness and conductance of contacts. We find that its Fourier transform $\tilde{C}(q)$ scales as a power of wavevector magnitude q: $\tilde{C}(q) \propto q^{-\mu}$ with $\mu = 2+H$ rather than the value $\mu = 2+2H$ reported previously. An analytic argument for $\mu = 2 + H$ is presented using the distribution of areas contained in disconnnected lakes or islands.

PACS numbers: 46.55.+d

1. Introduction

A wide variety of natural surfaces exhibit self-affine fractal roughness. Examples range from the earth's surface [1] to surfaces produced by fracture [2, 3] or growth [4, 5] to common machined surfaces [6, 7]. The geometrical properties of such surfaces have many practical implications and have been the focus of substantial research [1, 2, 3, 4, 5, 6, 7, 8, 9, 10, 11]. In this paper we consider contour cuts through self-affine surfaces, which are defined as the area where the height is below the contour level. The autocorrelation function for the contour cut area has received little attention, but is directly relevant to models of mechanical contact between surfaces [12, 13, 14].

The real area of intimate contact between surfaces plays a central role in theories of the friction and adhesion between solids [15, 16]. This contact area increases with applied load, but is usually confined to a miniscule fraction of the apparent area of the two surfaces. Both the total contact area and its spatial distribution profoundly affect interfacial properties such as the distribution of pressure, adhesion, electrical or thermal conductivity, and the leak rate of seals [15, 16, 17]. For example, at a fixed relative contact area, contact stiffness and interfacial heat conductivity will both be larger when the contact is spread out (leading to correlations at small wavevectors) than when contact occurs predominantly in the vicinity of the highest asperity [18, 19].

Calculations for the contact geometry have traditionally been based on the bearing area model [15, 20]. For a given surface separation, contact is assumed to occur wherever the initial, undeformed surfaces would interpenetrate. This is equivalent to the set of points $\mathbf{r}$ where the separation $h(\mathbf{r})$ between the initial undeformed surfaces is less than some threshold value h_0. Further approximations of the local surface profile as a sphere or ellipsoid are used to relate h_0 to the applied load in the widely used Greenwood-Williamson approximation [7, 21].

The set of points with $h < h_0$ corresponds directly to a contour cut at h_0. In addition to describing the bearing area model for contacts, contour cuts are relevant to topographical models, coinciding with the lakes on a self-affine surface with constant water level. The area under mountain peaks above some fixed height has the same scaling properties if the interface is symmetric about its midplane, as is the case for simple self-affine surfaces. Indeed, contact studies often assume that one surface is flat. Then $-h$ maps to the height of the rough surface and contact occurs at its peaks.

One measure of the geometry of contour cuts is the autocorrelation function $C(\Delta r)$. This is defined as the probability that two points separated by Δr both are in the contour cut (i.e. have $h < h_0$). The Fourier transform of this quantity, $\tilde{C}(q)$, decays algebraically with the magnitude of the wavevector q according to $\tilde{C}(q) \propto q^{-\mu}$. One can show that the autocorrelation function for contact stresses must scale with the same exponent μ [13] and this scaling plays an essential role in determining the elastic energy stored in contacts and the stiffness resisting deformation of contacts [19, 18, 22].

Our simulations show that μ does not depend on h_0, but does vary with the Hurst or roughness exponent H characterizing the scaling of the self-affine surface [23]. Our

numerical results are consistent with $\mu = 2 + H$, rather than the recently reported value of $2 + 2H$ [13]. This earlier work was primarily focussed on the very large difference between the bearing area model and full elastic calculations of the contact area where $\mu = 1 + H$ [13, 14]. The bearing area results in Ref. [13] were not extensively tested and we have discovered an analysis error that did not affect results reported for the full elastic calculation. The new numerical studies for the bearing area model reported here consider a wider range of H, system sizes, and h_0, and consistent results were obtained from two independent analysis programs. In addition, we present an analytic argument for $\mu = 2 + H$ based on known scaling properties of the sizes of "islands" or "lakes" on self-affine surfaces [8, 9, 10, 11, 24].

In the remainder of this paper, we will first provide the theoretical arguments in section 2, then present our new numerical data in section 3, and summarize in the final section 4.

2. Theory

The Hurst or roughness exponent H describes the scaling of the root mean squared (rms) change in height Δh with the lateral separation Δr. For a self-affine surface, $\Delta h \propto |\Delta r|^H$ with H between zero and unity. The familiar case of a random walk corresponds to $H = 1/2$ and most experimental and natural surfaces have larger H.

Contours of constant height on self-affine surfaces correspond to coastlines and have been extensively studied. Mandelbrot showed that the entire contour, including all disconnected loops, is a self-affine fractal with fractal dimension $2 - H$ [1]. The fractal dimension D_f of individual connected loops is smaller. Recent analytic and numerical arguments yield $D_f = (3 - H)/2$ [8, 9, 10].

The connected areas within disconnected contour loops correspond to the contacts or lakes that are of interest here and we will refer to them generically as clusters. While their boundaries are fractal, the clusters are two dimensional objects ‡[1]. While there may be holes within a cluster where the height exceeds the threshold (see for example Ref. [25]), the total area A scales as d^2 with d the diameter of the smallest circle that covers the cluster. The probability $P_A(A)$ that a cluster has a given area follows a power law

$$P_{\rm A}(A) \propto A^{-\alpha} \tag{1}$$

with $\alpha = 2 - H/2$ [8, 9, 10, 11, 26]. Note that all the above scaling properties are independent of the contour height and thus the fractional contact area. This is in sharp contrast to ordinary critical behavior where power law scaling only applies at a specific value of a control parameter.

‡ There may also be an infinite percolating cluster with different scaling properties. As discussed below, $\tilde{S}(q)$ is the same for filled and unfilled regions. One can then apply our analysis to whichever case does not have a percolating cluster. Note that because the clusters have a simple structure, the correlations within individual connected clusters are not very interesting, while the correlations for the total contour cut have nontrivial scaling.

The contact or lake correlation function can be written as

$$C(\mathbf{\Delta r}) \equiv \frac{1}{A_{tot}} \int d\mathbf{r} \Theta(h_0 - h(\mathbf{r})) \Theta(h_0 - h(\mathbf{r} + \Delta \mathbf{r})) \tag{2}$$

where the integral performs an average over the total surface area A_{tot} and the Heaviside function $\Theta(x)$ is 0 for $x < 0$ and unity for $x > 0$. The Fourier transform $\tilde{C}(q) = |\tilde{c}(q)|^2$, where $\tilde{c}(q)$ is the Fourier transform of $\Theta(h_0 - h(\mathbf{r}))$. Except at $q = 0$, $\tilde{C}(q)$ is identical to the correlation function for areas that are higher than h_0. This follows because $\Theta(h_0 - h(\mathbf{r})) + \Theta(h(\mathbf{r}) - h_0) = 1$, so the Fourier transforms of areas above and below h_0 are equal and opposite at nonzero q.

The contribution of a circular contact of radius a about the origin to $\tilde{c}(q)$ is

$$\tilde{f}_a(\mathbf{q}) = \frac{1}{2\pi} \int_0^a dr\ r \int_0^{2\pi} d\Phi\, e^{-iqr\cos\Phi} \tag{3}$$

$$= \frac{(qa)}{q^2} J_1(qa), \tag{4}$$

where we have used the properties of Bessel functions J_α of the first kind, specifically

$$J_0(u) = \frac{1}{2\pi} \int_0^{2\pi} d\Phi \exp(iu\cos\Phi) \tag{5}$$

and

$$uJ_1(u) = \int_0^u du'\, u' J_0(u'). \tag{6}$$

Clusters will not in general be circular, but despite their fractal boundaries and the presence of holes [25], they are two-dimensional objects [1]. As a result, the average contribution to $\tilde{c}$ of clusters of a given radius should exhibit approximately the same scaling with q as a circle. In particular, as in Eq. 4, $\tilde{f}(q)$ should be constant at small qa and drop rapidly at larger qa where a corresponds to the radius of a circle with the given cluster area A. This is all that is required for the following discussion.

The power law distribution of areas $P_A(A)$ implies a power law distribution of radii $P(a) = ca^{-2\alpha+1}$, where c is a constant. The total correlation function is approximated by an incoherent sum over patches of all sizes. One obtains

$$\tilde{C}(q) = \int_0^\infty da\, P(a)\, |\tilde{f}_a(\mathbf{q})|^2 \tag{7}$$

$$= c \cdot \int_0^\infty da\, a^{-2\alpha+1} \left\{ \frac{(qa)^2}{q^4} |J_1(qa)|^2 \right\} \tag{8}$$

$$= c \cdot \underbrace{\int_0^\infty d(qa)(qa)^{-2\alpha+1} \left\{ (qa)^2 |J_1(qa)|^2 \right\}}_{g(\alpha)} \cdot \underbrace{\frac{1}{q}\, q^{2\alpha-1}\, q^{-4}}_{q^{-(6-2\alpha)}} \tag{9}$$

$$= c \cdot g(\alpha) \cdot q^{-\mu}. \tag{10}$$

where

$$\mu = 6 - 2\alpha. \tag{11}$$

Note that $g(\alpha)$ is finite for $\alpha < 2$. Using the scaling relation $\alpha = 2 - H/2$ for areas of cuts through self-affine surfaces[8, 10, 11, 24], we obtain

$$\mu = 2 + H. \tag{12}$$

As shown below, Eq. 12 is consistent with our numerical results. It appears that adding contributions from different contacts incoherently is adequate because $\tilde{C}(q)$ is dominated by the largest clusters. Note that the real space correlation function for this μ is not well-defined unless a cutoff at a maximum wavelength and corresponding minimum wavevector q_{min} is introduced. The Fourier transform diverges as q_{min}^{-H} for all $r < 1/q_{min}$. The situation is very different for the contacts obtained from a full solution of the elastic contact problem. In this case, $\mu = 1 + H$, most of the area is in the smallest contacts, and correlations decay as $r^{-(1-H)}$. It also appears that the distribution of contact areas is cutoff more rapidly than a power law in the full elastic solution.

3. Results

In this work, two distinct algorithms have been used to generate self-affine surfaces. In both cases, heights are generated on a uniform, two-dimensional square grid with N points in each direction. The spacing a between points is taken as the unit of length. In the first method, fractal surfaces are constructed by generating Fourier coefficients $\tilde{h}(\mathbf{q}) = h_0 \cdot \mathrm{GRV}(\mathbf{q})/\mathrm{q}^{1+\mathrm{H}}$ on a two-dimensional square array. Here, h_0 is a constant, $\mathrm{GRV}(\mathbf{q})$ is a Gaussian-random-variable with random phase and $\tilde{h}(\mathbf{q}) = 0$. The height profile of the self-affine surface is then obtained by Fourier transforming $\tilde{h}(\mathbf{q})$ [23]. The constant h_0 is chosen to adjust the rms slope of the surfaces. The same technique was employed to build rough surfaces in Ref. [13].

The second approach for constructing self-affine surface topographies was the Voss or random midpoint displacement algorithm [27, 28], which has also been used by some of us in previous works [12, 26, 29, 30]. This is an iterative approach for generating heights for a self-affine fractal surface on a two-dimensional square grid. The process starts with a single square covering the entire system. At each iteration, each square is sub-divided into four smaller squares generating new corner points. Then height values for new corner points are assigned by adding the mean of the parent square corner heights to a Gaussian random value scaled by ℓ^H where ℓ is the distance between corners. This procedure is repeated until the required resolution is obtained as shown in Fig. 1(a) for a fractal surface with $N = 4096$ and Hurst exponent $H = 0.2$.

The contacts corresponding to the bearing area model are the set of grid points where $h < h_0$. As in Ref. [10], results for different realizations are compared at a fixed fraction f_c of contacting points rather than at fixed h_0. Fig. 1(a) shows an example for $f_c = 0.1$ and $H = 0.2$. A real space contact function $c(\mathbf{r})$ is defined by assigning 1 to all contacting points and 0 to all other points. This is then Fourier transformed to obtain $\tilde{c}(q)$ and squared to yield the desired correlation function $\tilde{C}(q)$.

We begin by examining $\tilde{C}(q)$ in the limit of small fractional contact area, since that is the most common case in experiments. Previous studies show that results for $f_c \leq 0.1$ are in this limit [26, 31]. Surfaces were constructed with $N = 8192$ and with roughness down to the grid spacing. A typical plot picturing the scaling of $\tilde{C}(q)$ for

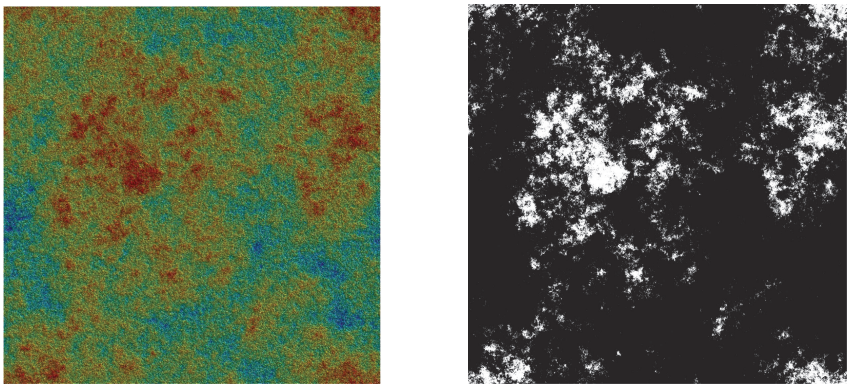

(a) Fractal surface (b) Contact area

Figure 1. Left: A fractal surface with $N = 4096$ points in each direction and $H = 0.2$. Color changes from red to blue with increasing height. **Right**: The contact area for a contour cut chosen to give a contact fraction of $f_c = 0.1$.

topographies characterized by different Hurst exponents and fractional contact areas is shown in Fig. 2. As derived in Ref. [13], normalizing by $f_c(1 - f_c)\tilde{C}(0)$ collapses the results for different contact areas onto universal curves. The straight lines in the figure show power law scaling with the predicted exponent $\mu = 2 + H$. The lines provide excellent fits at small q and the power law behavior extends to larger q as H increases.

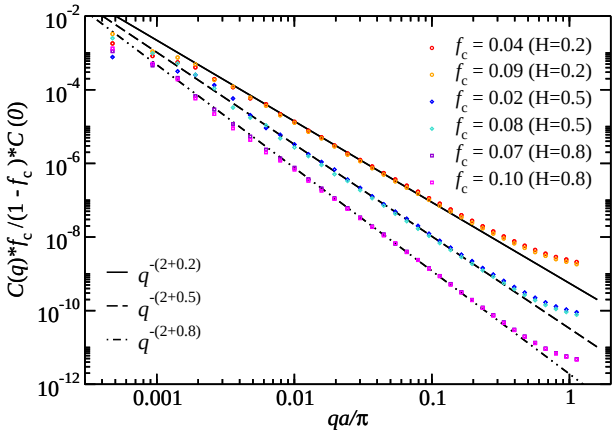

Figure 2. (Color online:) Normalized contact autocorrelation functions $\tilde{C}(q)$ corresponding to three values of the roughness exponent $H = 0.2, 0.5, 0.8$ and distinct fractional contact areas f_c. Surfaces were generated from Fourier components.

A comprehensive comparison of measured values of μ at different f_c and the analytic prediction $\mu = 2 + H$ is presented in Figure 3. It is evident from the results for $f_c = 0.6$, that the same power law is observed outside of the dilute limit. For these data, surfaces with $N = 8192$ and H ranging from 0.2 to 0.9 were generated with the random

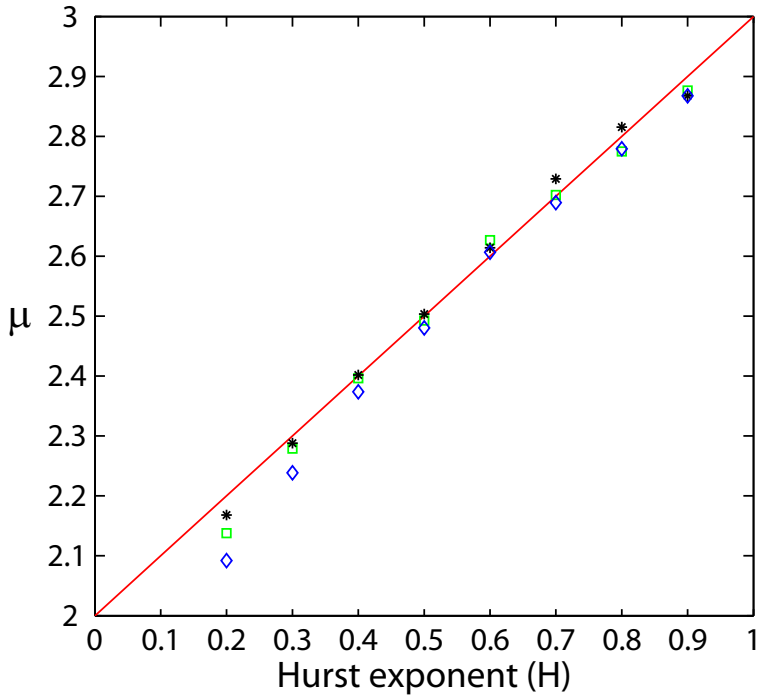

Figure 3. (Color online:) Comparison between theoretical prediction (line) and numerical results for the power law exponent μ describing the contact autocorrelation function. Numerical results are for a grid with $N = 8192$ and fractional contact area of 10% (squares and diamonds) or 60% (asterices) and were obtained from least mean squares fits over $0.008 \leq qa \leq 0.8$ (diamonds) or $0.008 \leq qa \leq 0.4$ (squares and asterices). Statistical errors in the fits are comparable to the symbol size. Systematic errors increase as H goes to 0 or 1.

midpoint algorithm. A least mean squares fit was performed over two different ranges of wavevector to demonstrate the sensitivity of the fits to the upturn in $\tilde{C}(q)$ seen at large q in Fig. 2. Decreasing the upper end of the fit from $\pi/2$ to $\pi/4$ provides a substantial improvement, particularly at low H where Fig. 2 shows greater curvature. Exponents obtained from the surfaces generated with the Fourier method were equivalent within our numerical uncertainty of about 0.02 at $H = 0.5$ and 0.05 at large and small H. Within this uncertainty the numerical results are consistent with $\mu = 2 + H$.

The analytic argument presented in section 2 assumed continuous circular contact areas, while the area is discretized onto nodal points in the numerical calculation. As H decreases, the exponent for the area distribution in Eq. 1, $\alpha = 2 - H/2$, increases and more and more of the clusters contain only a few nodes. To evaluate the influence of this effect, we examined surfaces where roughness only extended to a wavelength $l_{\min}$ that was larger than the node spacing a. This makes the representation of the area more continuous, but did not produce any statistically significant change in μ.

Another type of error becomes more important at large H. Since α is larger, the total number of contacts decreases and an increasing fraction of the area is in a few large clusters. The reduced statistics lead to the larger errorbars for $H = 0.9$.

We have also studied the case of rough two-dimensional solids. Here the contour cuts reduce to lines between points where the interface has a given height. Our numerical results for the autocorrelation of these lines are consistent with $\mu = 1 + H$ over the entire range of H considered. Once again, this value is higher than the value of $\mu = H$ obtained for calculations of contact correlations that treat the full elastic deformation of the substrate numerically [32] or analytically [14]. It is interesting that in both 2D and 3D the full calculation reduces μ by unity.

4. Conclusions

In this paper we have examined the Fourier transform $\tilde{C}(q)$ of the autocorrelation function of areas within contours of constant height on self-affine fractal surfaces. These correspond to the contact areas in the widely used bearing area model that assume contact between two solids occurs where the initial separation of the two rough, non-contacting surfaces is below a given threshold value. The contour cuts also correspond to the lakes at constant water level on a fractal landscape or the peaks above a fixed height.

Numerical results show an algebraic decay of correlations $\tilde{C}(q) \propto q^{-\mu}$. We presented an approximate analytic argument that predicts $\mu = 2 + H$. Numerical results for surfaces with Hurst exponent $0.2 \leq H \leq 0.9$ and generated with different algorithms at different fractional contact areas (0.1% to 60%) are consistent with the analytic prediction within our statistical errors. These are largest for small H where the scaling range is smaller.

A previous paper [13] had reported a larger value of $\mu = 2 + 2H$, but a simple analysis error was found in the code used to study the bearing area model in that work, motivating the preparation of this article. The error did not affect the results in Ref. [13] for contact areas obtained from a full numerical solution of the elastic contact problem. The full elastic solution yields a very different decay $\mu = 1+H$ [13], which has also been derived from Persson's contact theory [14]. This change in exponent means that the bearing area model produces contacts with very different geometry than the full elastic calculation. For example, almost all the area is in the largest contacts for the bearing area model and almost all the area is in the smallest contacts for the full calculation [26, 13]. The real space correlation function $C(\Delta r)$ decays as r increases for the full calculation but grows with r for the bearing area approximation. These differences may lead to discrepancies between experiment and predictions based on the bearing area model.

Acknowledgements: This material is based on the work supported by the Swiss National Foundation under Grant no 200021_122046/1, the European Research Council Starting Grant no 240332 and the Air Force Office of Scientific Research under grant AFOSR FA9550-0910232.

5. References

[1] B. B. Mandelbrot. *The Fractal Geometry of Nature*. Freeman, New York, 1982.

[2] E. Bouchaud. Scaling properties of cracks. *J. Phys. Conden. Matter*, 9:4139–4344, 1997.

[3] D. Bonamy, L. Ponson, S. Prades, E. Bouchaud, and C. Guillot. Scaling exponents for fracture surfaces in homogeneous glass and glassy ceramics. *Phys. Rev. Lett.*, 97:135504, 2006.

[4] P. Meakin. *Fractals, scaling and growth far from equilibrium*. Cambridge, Cambridge, 1998.

[5] J. Krim and G. Palasantzas. Experimental observation of self-affine scaling and kinetic roughening at sub-micron lengthscales. *Int. J. of Modern Phys. B*, 9:599–632, 1995.

[6] J. F. Archard. *Proc. R. Soc.*, A243:190, 1957.

[7] J. A. Greenwood and J. B. P. Williamson. *Proc. R. Soc. London*, A295:300, 1966.

[8] J. Kondev and C. L. Henley. *Phys. Rev. Lett.*, 74:4580, 1995.

[9] J. Kondev, C. L. Henley, and D. G. Salinas. Nonlinear measures for characterizing rough surface morphologies. *Phys. Rev. E*, 61:104–125, 2000.

[10] Z. Olami and R. Zeitak. Scaling of island distributions, percolation, and criticality in contour cuts through wrinkled surfaces. *Phys. Rev. Lett.*, 76:247–250, 1996.

[11] M. A. Rajabpour and S. M. Vaez Allaei. *Phys. Rev. E*, 80:011115, 2009.

[12] S. Hyun and M. O. Robbins. *Tribol. Int.*, 40:1413, 2007.

[13] C. Campañá, M. H. Müser, and M. O. Robbins. *J. Phys.: Condens. Matter*, 20:354013, 2008.

[14] B. N. J. Persson. *J. Phys.: Condens. Matter*, 20:312001, 2008.

[15] F. P. Bowden and D. Tabor. *Friction and Lubrication*. Wiley, New York, 1956.

[16] B. N. J. Persson. *Sliding Friction: Physical Principles and Applications*. Springer, Berlin, 2 edition, 2000.

[17] B. Lorenz and B. N. J. Persson. Leak rate of seals: Comparison of theory with experiment. *Europhys. Lett.*, 86:44006, 2009.

[18] J. R. Barber. Bounds on the electrical resistance between contacting elastic rough bodies. *Proceedings of the royal society of london series A-Mathematical physical and engineering sciences*, 459(2029):53–66, JAN 8 2003.

[19] C. Campaña, B.N.J Persson, and M.H. Müser. Transverse and normal interfacial stiffness of solids with randomly rough surfaces. *Journal of Physics: Condensed Matter*, 23:085001, 2011.

[20] J. A. Greenwood and J. J. Wu. Surface roughness and contact: An apology. *Meccanica*, 36:617–630, 2001.

[21] A. W. Bush, R. D. Gibson, and T. R. Thomas. *Wear*, 35:87, 1975.

[22] S. Akarapu, T. Sharp, and M.O. Robbins. Stiffness of contacts between rough surfaces. *arXiv*, (10.1479v1), 2010.

[23] P. Meakin. *Fractals, scaling and growth far from equilibrium*. Cambridge University Press, New York, 1977.

[24] J. C. Russ. *Fractal surfaces*. Springer, 1994.

[25] P. R. Nayak. Some aspects of surface roughness measurement. *Wear*, 26(2):165–174, 1973.

[26] S. Hyun, L. Pei, J. F. Molinari, and M. O. Robbins. *Phys. Rev. E*, 70:026117, 2004.

[27] R. F. Voss. *Fundamental Algorithms in Computer Graphics*. Springer-Verlag, Berlin, 1985.

[28] D. Saupe et al. H. O. Peitgen. *The Science of Fractal Images*. Springer, 1st edition, 1988.

[29] G. Anciaux and J. F. Molinari. Contact mechanics at the nanoscale, a 3d multiscale approach. *International Journal for Numerical Methods in Engineering*, 79, no. 9:1041–1067, 2009.

[30] G. Anciaux and J. F. Molinari. Sliding of rough surfaces and energy dissipation with a 3d multiscale approach. *International Journal for Numerical Methods in Engineering*, 83, no. 8:1255–1271, 2010.

[31] C. Campañá and M. H. Müser. *Europhys. Lett.*, 77:38005, 2007.

[32] Binquan Luan and Mark O. Robbins. Hybrid atomistic/continuum study of contact and friction between rough solids. *TRIBOLOGY LETTERS*, 36(1):1–16, 2009.